MEDIUM SCALE EXPERIMENTS ON STABILIZING RISER SLUG FLOW

Heidi Sivertsen * Vidar Alstad ** Sigurd Skogestad,[1]

Department of Chemical Engineering, Norwegian University of Science and Technology, Trondheim, Norway

** Current affiliation: StatoilHydro, Stjørdal, Norway*

*** Current affiliation: StatoilHydro Research Centre, Porsgrunn, Norway*

Keywords: Process control, multiphase flow, dynamic simulation, petroleum, riser slugging, controllability analysis

Author to whom correspondence should be addressed:

skoge@chemeng.ntnu.no

This is the second of two papers describing control experiments on different scale slug rigs. The first paper describes experiments performed on a small-scale lab rig build at NTNU (Norwegian University of Science and Technology) Department of Chemical Engineering. These experiments showed that despite noisy measurements, it is possible to stabilize the flow in the slug flow region using only topside measurements. The question to be answered in this paper is; do these results also apply for *larger* riser-systems?

In this paper, we look at some results obtained from a 10m high, 3 in. diameter *medium*-scale test rig located at StatoilHydro Research Centre in Porsgrunn, Norway. Several cascade control structures are tested and compared; both with each other and the results obtained from the small-scale NTNU loop. The rig was also modelled and analysed using a simple three-state model.

The new experiments were successful and confirmed the results achieved using the small-scale rig. This suggests that the small-scale lab loop can be used as a tool to predict possible useful control strategies for the riser slug problem.

1. INTRODUCTION

The behavior of multiphase flow in pipelines is of great concern in the offshore oil and gas industry, and a lot of time and effort have been spent studying this phenomena. The reason for this is that by doing relatively small changes in operating conditions, it is possible to change the flow behavior in the pipelines drastically. This has a huge influence on important factors such as productivity, maintenance and safety.

Active control makes it possible to avoid the slug flow regime with conditions where slug flow is predicted. This way it is possible to operate with the same average flow rates as before, but without the huge oscillations in flow rates and pressure. The advantages with using active control are large; it is much cheaper than implementing new equipment and it also removes the slug flow all together thereby removing the strain on the system. This way a lot of money can also be saved on maintenance. Also, it is possible to produce with larger flow rates than what would be possible by manually choking the topside valve.

Several experiments were performed to test similar control configurations as was also tested on the NTNU small-scale lab rig. This was done in order to investigate whether different scales have an effect on the quality of the control structures. Having results from a larger scale rig could give an indication on whether the small-scale

NTNU lab rig really was suitable as a tool for finding good control solutions to be used in larger scale facilities, such as an offshore production system.

The question was; could active control be used to stabilize the flow also for the medium-scale lab rig? In particular, it was interesting to see whether only topside measurements could be used to stabilize the flow, as was done on the small-scale lab rig described in **Sivertsen et al. (2009).**

2. EXPERIMENTAL SETUP

Earlier studies on using only topside measurements are found in **Godhavn et al. (2005)** where experiments were performed on a larger rig and the flow was controlled using combinations of pressure and density measurements. The results were, however, not compared with what is obtainalble using subsea measurements in the control structure. Similar experiments as the ones described in this paper were earlier performed on a small-scale lab rig. These experiments are described in Sivertsen et al. (2009).

The medium-scale multiphase flow control rig at StatoilHydro Research Centre in Porsgrunn is built to simulate multiphase flow in an offshore well/pipeline and production unit. The facility is ideal for development and testing of new control solutions for anti-slug and separator control under realistic conditions. **Fig. 1** shows a photograph of the facility.

Fig. 1 - A birds-view perspective of the medium-scale riser rig at StatoilHydro Research Centre in Porsgrunn,
Located in Figure 1.eps

During the experiments the flow consisted of water and air. The pipe diameter is 3 in. (7.6 cm) and the height of the riser is approximately 10 m. The inflow of gas and water was pressure dependent. Water inlet rate during the experiments was 7 to 8 m^3/h while the air inflow rate fluctuated between 8 to 11 m^3/h. Slugging occurred for valve openings larger than about 12%. **Fig. 2** show a schematic overview of the layout and available instrumentation.

Fig. 2 - Schematic overview of the layout and available instrumentation,
Located in Figure 2.eps

The loop includes an approximately 4 m long section where gas, oil and water are introduced through different inlets. This ”well section” consists of annulus and tubing, a 15.2 cm diameter outer pipe and a 7.6 cm diameter inner tubing with perforations.

The pipe section consist partly of flexible tubing, hence it is possibly to vary the geometry of the piping. This way the inclination of the riser and other parts of the pipe can be adjusted to achieve the desired geometry.

The pipeline geometry during the experiments was chosen to give terrain-induced slugging. A more detailed schematic of the geometry used in the experiments is shown in **Fig. 3.** The numbers indicate the location of feeding inlets and important instrumentation.

Fig. 3 - Schematic of the geometry of the riser-system,
Located in Figure 3.eps

The numbers 1, 2 and 3 indicate the air, water and oil inlets respectively. Downstream this section the pipeline is close to horizontal for about 10 m. An approximately 7 m, 35˚ inclined section then follows. A pressure measurement (P_1) is implemented at the end of this section (4). The next 60 m section has a 1.8˚ declination, followed by an approximately 20 m horizontal section with a pressure and temperature measurement at the end (6). A 10 m long vertical riser then follows a low point in the geometry (7). The low-point contains a see-trough section, which makes it possible to determine visually the flow regime in this section. At the top of the riser a production choke (10) and separator (11) are located. There is also a pressure measurement (8) and a see-through section (9) located half-way up the riser. Upstream the production choke a pressure measurement (P_2) and a gamma densiometer are implemented.

The water and oil outlets from the separator are returned to a large 10 m^3 buffer tank. The oil and water feed are pumped from this buffer tank back to the respective phase inlets in the well section using two displacement pumps. Before entering the well section, the feed flow rate and density of each phase are measured.

2.1 Gas feed

The compressed air is supplied from the local air supply net. The supplied air holds a pressure of approximately 7 bara. An automated control valve controls the feed flow rate of compressed air to the well section. The operating range of the control valve is 10 to 400 kg/h.

The mass flow and the density of the compressed air are measured using a Coriolis type mass flow meter.

2.2 Water feed

A displacement pump controls the feed flow rate of water. The power is either set directly by the operator or given as output from a feedback controller using the volumetric flow rate as measurement. The pressure and single-phase flow rates are measured downstream the pumps, using a differential pressure volumetric flow meter (Pivot tube) for the air and a Coriolis type mass flow for the water.

2.3 Separator

The three-phase separator located at the top of the riser has a volume of approximately 1.5 m^3. A 53 cm high weir plate separates the oil and water outlets. The separator is equipped with a pressure measurement and measurements of the oil and water levels. No oil was added to the flow during the experiments presented in this paper.

2.4 Control choke valve

The control choke valve is a vertically positioned valve located at the top of the riser. The valve is equipped with a Profibus-PA Positioner, which returns the actual valve position to the control system.

2.4.1 Choke valve characteristics

Several flow experiments had been performed in order to find the single- and two-phase (water/air) valve characteristics:

$$F_Q = \overbrace{C_v f(z)}^{K(z)} \sqrt{\frac{\Delta P}{\rho}} \tag{1}$$

C_v is the valve constant and $f(z)$ is the characteristics of the valve. ΔP is the pressure drop across the valve and ρ is the density of the fluid. For valve openings less than 50% and 60% for single-phase and two-phase flow respectively, the characteristics were found to be close to linear. Thus, **Eq. 1** can be written

$$F_Q / C_v = z\sqrt{\frac{\Delta P}{\rho}} \quad (2)$$

Values for F_Q/C_v can be calculated from given values for valve opening z, measured pressure drop across the valve ΔP and measured density ρ.

2.5 Instrumentation

A number of automatic control valves are installed. This includes the production choke valve, the valves controlling gas, water and oil outlet from the separator and the feed flow of air to the well section. These valves can be operated either in manual mode or in automatic mode where valve openings are given as output from PID feedback controllers. The rig is controlled from a control room located close to the rig.

3. Controllability analysis

3.1 Modelling

In Sivertsen et al. (2009) it was shown how an analysis of a model describing a *small*-scale lab-rig did reveal fundamental control limitations depending on which measurements that were used for control. This was found using a simplified model **(Storkaas et al. (2003)).** One of the advantages of this simple model is that it is well suited for controller design and analysis. It consists of three states; the holdup of gas in the feed section (m_{G1}) and in the riser (m_{G2}), and the holdup of liquid (m_L). The model is illustrated in **Fig. 4.**

The same model was used to predict the behaviour for the medium-scale lab rig used in this study. Using this model the system was analysed in the same way as in Sivertsen et al. (2009). Both open- and closed loop simulations were performed.

Fig. 4 - Storkaas' pipeline-riser slug model (Storkaas et al. (2003)),
Located in Figure 4.eps

After entering the geometrical and flow data for the lab rig, the model was tuned as described in Storkaas et al. (2003) to fit the open loop behaviour of the lab rig. The model data and tuning parameters are presented in **Table 1**. After inserting new system parameters and re-tuning the model, the open-loop data found using the model fitted the experimental results quite well as shown by the bifurcation plot in **Fig. 5.**

Table 1 - Model data parameters,

Located in Tables.doc

The bifurcation diagram gives information about the valve opening for which the flow becomes unstable and shows the amplitude of the pressure oscillations for the inlet and topside pressures (P_1 and P_2). The upper lines in the bifurcation plot show the maximum pressure at a particular valve opening and the lower line shows the minimum pressure. The lines meet at the "bifurcation point" when the valve opening is approximately 12%. This is the point where transition to slug flow occurs naturally and this is the highest valve opening which gives "non-slug" behaviour in open-loop operation, without control. The dotted line in the middle shows the unstable "non-slug" solution predicted by the model. This is the desired operating line with closed-loop operation.

Fig. 5 - Bifurcation plot for the medium scale rig: Pressures at inlet P_1 and topside P_2 as function of choke valve opening z,

Located in Figure 5.eps

The bifurcation plot was obtained by open-loop simulations of the system at different valve openings. Some of these results are plotted in **Fig. 6** together with experimental results. The model fit the experimental data quite well, in terms of both amplitude and frequency of the oscillations. Note that a shift in time does not matter. The match between simulated and experimental results is especially very good for a valve opening of 14.9%.

In **Fig. 7** a root-locus diagram of the system is plotted. This shows how the poles, computed eigenvalues from the model, cross into the RHP (Righ Half Plane) of the imaginary plane as the valve opening reaches 12% from below. This confirms what was seen in the bifurcation diagram.

Fig. 6 - Open loop data for valve openings 10, 15, 20 and 25%,

Located in Figure 6.eps

Fig. 7. Root-locus plot showing the trajectories of the RHP open-loop poles when the valve opening varies from 0 (closed) to 0.4,

Located in Figure 7.eps

3.2 Analysis

The model can now be used to explore different measurement alternatives for controlling the flow. The following measurements were analysed in this study; inlet pressure P_1, pressure upstream production choke P_2, density ρ, mass flow rate F_W and volumetric flow rate F_Q through the topside choke. **Fig. 8** shows the different measurement candidates.

Fig. 8 - Measurement candidates for control,

Located in Figure 8.eps

In Sivertsen et al. (2009) it was shown for the small scale lab rig how the RHP poles and zeros and their locations compared to each other in the imaginary plane had a large influence on the controllability of the system. By scaling the system and calculating the sensitivity peaks, it is possible to get a picture of the challenges in terms of stabilizing the system.

The analysis is described in **Appendix A**. It shows that we might expect problems due to RHP pole/zero location when using a topside density measurement or pressure as single measurements for control. In addition, the analysis discover that we might experience problems due to drift (low steady state stationary gain) when using topside flow measurements. These are similar results as was found for the small-scale lab rig in Sivertsen et al. (2009).

3.3 Simulations

Closed-loop simulations were performed in order to investigate the effect of the limitations found in the analysis. The measurements were used as single measurements in a feedback loop with a PI-controller. **Fig. 9** shows this control structure using the inlet pressure P_1 as measurement.

Fig. 9 - Feedback control using PI controller with inlet pressure P_1 as measurement,

Located in Figure9.eps

Fig. 10 compares the simulation results obtained using four different measurement candidates. Disturbances in inlet flow rates for the gas and water are not included in the simulations. The results can for this reason differ somewhat from the results obtained in Sivertsen et al. (2009). Despite this, the results were quite similar. Results

using the topside pressure P_2 are not included in the plot, as the corresponding controller was not able to stabilize the flow.

Fig. 10 - Stabilizing slug flow using the choke valve (z); PI control with four alternative measurements, Located in Figure10.eps

At first, the controllers are turned off and the system is left open loop for approximately three and a half min. with a valve opening of 20%. From the bifurcation diagram in Fig. 5 it was shown that the system goes unstable for valve openings larger than 12%. As expected the system oscillates due to the presence of slug flow.

When the controllers are activated the control valves start working as seen from the right plot in Fig. 10. After about 80 min. the set points are changed for all the controllers, bringing the flow further into the unstable region. The aim of the simulation study is to be able to control the flow with satisfactory performance as far into the unstable region as possible, which means with as high average valve opening as possible. Several simulations were performed, and the ones stabilizing the flow at the highest valve opening are presented in Fig. 10.

As in Sivertsen et al. (2009), the controllers giving the best results were the ones using inlet pressure P_1 and volumetric flow rate F_Q as measurements. However, this time the flow controller F_Q outperformed the pressure controller, being able to stabilize the flow with an average valve opening of impressing 55%. Based on earlier knowledge of slug control and experimental results; these results are too good to be true, and might come from the fact that no disturbances in the inlet flow rates were added in the simulations this time.

The results using the density and mass flow controller were quite similar to those obtained for the small scale lab rig in Sivertsen et al. (2009). It was possible to control the flow in the unstable region, but the controllers were slow and did not manage to stabilize the flow very far into the unstable region. The analysis in Appendix A indicates that these problems stems from the RHP zeros introduced when using these measurements.

4. Experimental results

The analysis and simulations in Sec. 3 showed that both the inlet pressure P_1 and the scaled topside volumetric flow rate F_Q were suitable for stabilizing the flow. The results using the topside density ρ were not as good as for P_1 and F_Q, but still it was possible to control the flow using also this measurement.

Looking at Table A-2 in Appendix A it is clear that except for the mass flow measurement F_W with zero steady-state gain, ρ is the measurement having the lowest steady-state gain at valve opening 20%. Also for the volumetric flow rate measurement F_Q the steady-state gain is quite low for valve opening 20%, and we might expect the same problems using this measurement as the single measurement.

Control configurations using *combinations* of measurements can improve the performance of a controller when compared to controllers using single measurements. In order to avoid the drift problem, different cascade controllers were tested experimentally. Six cascade controllers with different measurement combinations were tested.

The measurements were combined in a cascade control configuration, where the set point for the inner controller is adjusted by the outer loop to prevent the inner controller from drifting. This way ρ and F_Q can be used as measurement in an inner loop, even though the controller based solely on one of these measurements suffer from the drift problem. The volumetric flow measurement used during the experiments was scaled with respect to the choke valve constant C_v.

Topside measurements are often noisy, and so also in this case. For this reason the density measurement signal was filtered using a first-order low-pass filter with a time constant of 4s.

Additional experiments were performed using the inlet pressure P_1 as measurement for the inner loop. Although P_1 is not a topside measurement, and often not available in many real subsea applications, it was included to serve as a comparison for the other controllers. As outer measurements, the pressure drop across the control valve P_2 and topside choke valve opening z were used. This gives all together six combinations of measurements in the outer and inner loop respectively; (a) z and P_1 (b) z and ρ (c) z and F_Q (d) P_2 and P_1 (e) P_2 and ρ (f) P_2 and F_Q. **Fig. 11** shows a sketch of a cascade control structure for alterative (e) and **Figs. 12-14** shows the experimental results for all six alternatives. In Figs. 12-14, plot (a) shows the results when valve opening z is used as outer loop measurement. In plot (b) the measured topside pressure P_2 is used.

Fig. 11 - Cascade control with measurements density ρ (inner loop) and pressure drop across topside valve P_2 (outer loop),

Located in Figure11.eps

Fig. 12 - Experimental results using P_1 in the outer loop and a) z and b) P_2 in the inner loop,

Located in Figure12a-12b

Fig. 13 - Experimental results using ρ in the outer loop and c) z and d) P_2 in the inner loop,

Located in Figure13a-13b

Fig. 14 - Experimental results using F_Q in the outer loop and e) z and f) P_2 in the inner loop,

Located in Figure14a-14b

During the experiments, the operation is gradually moved further into the unstable region by changing the set point in the outer loop (increasing z_S and decreasing $P_{2,S}$). The valve opening for which the flow can no longer be stabilized gives a measure on the performance of each controller. Note that being able to increase the mean valve opening and at the same time keep the flow stable has large economic advantages. This is because producing at a higher valve opening implies less friction loss and increased production.

The results using all of the controllers were very good, and they all managed to stabilize the flow far into the unstable region. The upper plot in each of the subfigures shows how the valve opening is increased during the experiments.

Table 2 compare the average values the last 12 min before the controllers go unstable. As mentioned, the mean valve opening gives a good indication of the quality of the controller. See also **Fig. B-1** in **Appendix B** which shows more detailed plots for all the controllers the last 12 min. before instability.

Table 2 - Mean values just before instability using different cascade controllers, based on data plotted in Fig. B-1,

Located in Tables.doc

Based on the results, we conclude that using P_2 in the outer loop and either P_1 or F_Q in the inner loop is the best choice with average maximum valve opening 23.8% and 23.9%, respectively. The third best choice is using z in the outer loop and F_Q in the inner loop (22.8%).

The controllers were not fine-tuned and the results might for this reason be influenced somewhat by the quality of the tuning. Still, the results showed that it was possible to stabilize the flow very well using only topside measurements and that these results are comparable to the results found when including subsea measurement P_1 as one of the measurements.

5. Discussion

It is important to note that Storkaas' model used to analyze the system is a very simplified model, and it was used merely as a tool to see which problems might occur in the lab, and the underlying reasons for the problems. When comparing the experimental results with analysis and simulations using Storkaas' model prior to the experiments, it was clear that the experimental results were far better than the model predicted when using the density as measurement. The model is, however, not very detailed and it is merely used as a tool to understand the underlying dynamics of the problem.

The pressure dependency of the inflow rates of gas and water was not included, and the effect of this dependency probably helps to stabilize the flow since the inlet rates are decreased as more water accumulates in the riser.

During the experiments the timing for when the controller is activated (where in the slug-cycle) was very important for the controller's ability to stabilize the flow. When the controller was activated just after the inlet pressure had peaked, the controller managed to stabilize the flow quite easily. If the controller was activated at some other time, usually the controller didn't manage to stabilize the flow at all.

Also, the tuning of the controllers has a big influence on the results. Even better results might be achieved with other types of controllers or better tuning. This is also why it is not possible to make a clear recommendation of which combination of measurements is best. The study does, however, show that all the combinations stabilize the flow quite well.

6. Conclusions

This paper has presented results from a medium-scale riser rig where the aim was to control the flow using only topside measurements. The results show that it was possible to stabilize the flow using different combinations of topside measurements. Table 2 shows the different controller results compared to each other. The best results were achieved with the scaled volumetric flow rate F_Q/C_v as the inner measurements, although this result may be dependent on the tuning of the controllers. All of the controllers managed to stabilize the flow well, increasing the maximum valve opening from 12% without control to more than 20% with control.

When comparing the results with similar experiments performed on a small-scale riser rig build at our department (Sivertsen et al. (2009)), the results using different control configurations are quite similar. This suggests that the small-scale riser rig might be suitable for testing different control strategies prior to more costly and time-consuming tests on larger rigs.

Acknowledgments

The authors would like to thank StatoilHydro Resarch Centre in Porsgrunn for letting us do experiments on their test facilities. Also we appreciate all the help that was provided by the people working there, in particular Kristin Hestetun for helping with the experiments. Also the technical staff deserves thanks for helping with the equipment.

Abbreviations

DC	Density controller (Fig. 10)
DI	Density measuring instrumentation (Fig. 3)
DT	Density measurement transmitter (Fig. 10)
dP, ΔP	Pressure drop
F_Q, Q	Volumetric flow rate
F_W	Mass flow rate
LI	Separator level measuring instrumentation (Fig. 3)
NTNU	Norwegian University of Science and Technology
P_1	Pressure upstream the riser
P_2	Topside pressure
PC	Pressure controller (Fig. 11)
PI	Pressure measuring instrumentation (Fig. 3)
PI control	Proportional, Integral controller
PID control	Proportional, Integral, Derivative controller
PT	Pressure measurement transmitter (Fig. 10)

RHP	Righ Half of the imaginary Plane
z	Valve opening
ρ	Density

Appendix A - Modeling and analysis

The process model G and disturbance model G_d were found by linearizing Storkaas' model at two operation points (z = 0.15 and z = 0.2). The process variables were scaled with respect to the largest allowed control error and the disturbances were scaled with the largest variations in the inlet flow rates in the lab, as described in **Skogestad and Postlethwaite (1996)**. The disturbances were assumed to be frequency independent. The input was scaled with the maximum allowed positive deviation in valve opening since the process gain is smaller for large valve openings. For measurements y=[P_1 P_2 ρ F_W F_O] the scaling matrix is D_e=diag[*0.1bar 0.1bar 50kg/m*^{3} *0.2kg/s 1e*$^{-3}$*m*^{3}*/s*]. The scaling matrix for the disturbances d=[m_G *and* m_L] is D_d= diag [*2e*$^{-3}$*kg/s 0.2kg/s*]. The nominal values are 0.0075 kg/s for the gas and 1.64 kg/s for the water rate. The input is scaled D_u=1-z_{nom} where z_{nom} is the nominal valve opening.

Tables A-1 and **A-2** summarize the results of the analysis. The locations of the RHP poles and zeros are presented for valve openings 15 and 20%, as well as stationary gain and lower bounds on the closed-loop transfer functions described in Sivertsen et al. (2009). The pole location is independent of the input and output (measurement), but the zeros may move. From the bifurcation plot in Fig. 5, it is seen that both of these valve openings are inside the unstable area. This can also be seen from the RHP location of the poles.

Table A-1 - Control limitation data for valve opening 15%. Unstable poles at *p=0.0062±0.060i.*

Located in Tables.doc

Table A-2 - Control limitation data for valve opening 20\%. Unstable poles at *p=0.0190±.073i.*

Located in Tables.doc

The only two measurements of the ones considered in this paper which introduces RHP-zeros into the system, are the topside density ρ and pressure P_2. The RHP zeros are in both cases located quite close to the RHP poles, which results in the high peaks especially for sensitivity function *SG* but also for *S*. In **Fig. A-1** the RHP poles

and relevant RHP zeros are plotted together. This plot shows that we can expect problems when trying to stabilize the flow using these measurements as controlled variables.

Fig. A-1 - Plot-zero map for valve opening 20%,

Located in FigureA1.eps

The model is based on constant inlet flow rates. The stationary gain for F_W predicted by the model is 0, which means that it is not possible to control the steady-state behavior of the system and the system will drift. Usually the inlet rates are pressure dependent, and the zeros for measurements F_Q and F_W would be expected to be located further away from the origin than indicated by Tables 2 and 3.

Fig. A-2 - Bode plots for the plant models using different measurements,

Located in FigureA2.eps

Fig. A-3 - Bode plots for the disturbance models using different measurements,

Located in FigureA3.eps

Figs. A-2 and A-3 show the Bode plots for the different plant models and disturbance models respectively. The models were found from a linearization of the model around valve opening 15%. As in Sivertsen et al. (2009) the Bode plots show that for the mass flow rate measurement F_W the low frequency value of the disturbance model $|G_dW|$ is higher than plant model $|G_W|$. For acceptable control we require $|G(jw)| > |G_d(jw)|-1$ for frequencies where $|G_d|>1$ (Skogestad and Postlethwaite (1996)). In this case $|G_d(0)|$ is 1.01 and G_W is close to zero, which means problems can occur for this measurement.

Appendix B - Experimental results

a) P_1 and z

b) ρ and z

c) F_Q/C_v and z

d) P_1 and P_2

e) ρ and P_2

f) F_Q/C_v and P_2

Fig. B-1 - Experimental results using six different combinations of measurements, last 12 min before instability, Located in FigureB-1a-B-1f.eps

References

J.M. Godhavn, M.P. Fard, and P.H. Fuchs. 2005.New Slug Control Strategies, Tuning Rules and Experimental Results. *Journal of Process Control, 15(15):547– 577*

H. Sivertsen, E. Storkaas and S. Skogestad. 2009. Small Scale Experiments on Stabilizing Riser Slug Flow. *To be published.*

S. Skogestad and I. Postlethwaite. 1996. *Multivariable Feedback Control.* John Wiley & sons

E. Storkaas, S. Skogestad, and J.M. Godhavn. 2003. A Lowdimentional Model of Severe Slugging for Controller Design and Analysis. *Multiphase '03, San Remo, Italy, 11-13 June 2003*

List of Figures

List of Tables

Figure 1

Figure 2

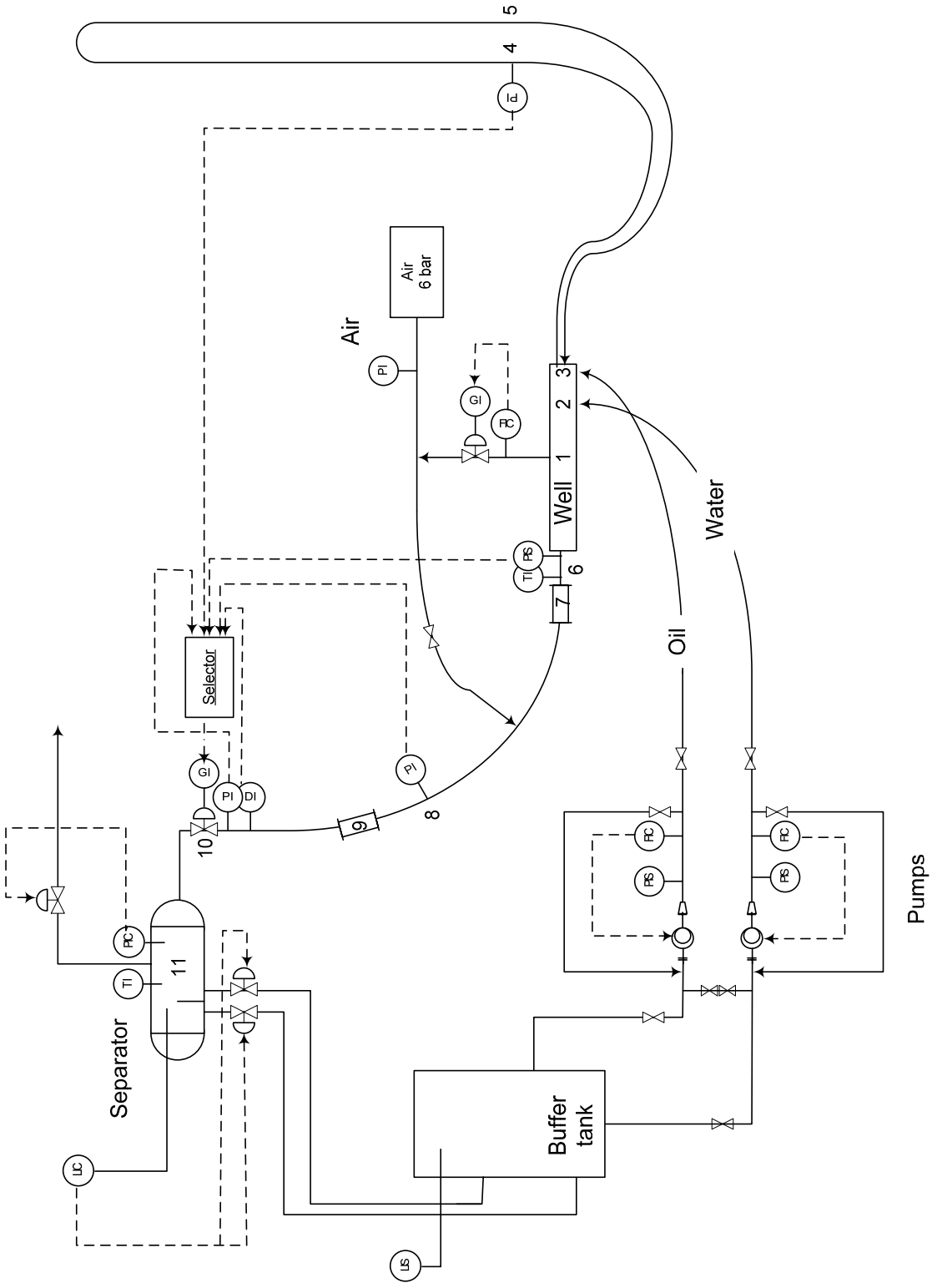
5
4
PI
Air
6 bar
Air
PI
GI
PIC
1
2
3
Well
Water
Oil
TI
PIS
6
7
Selector
GI
PI
DI
PI
8
9
10
PIC
TI
11
Separator
LIC
LS
Buffer
tank
PIC
PIS
PIC
PIS
Pumps

Figure 3

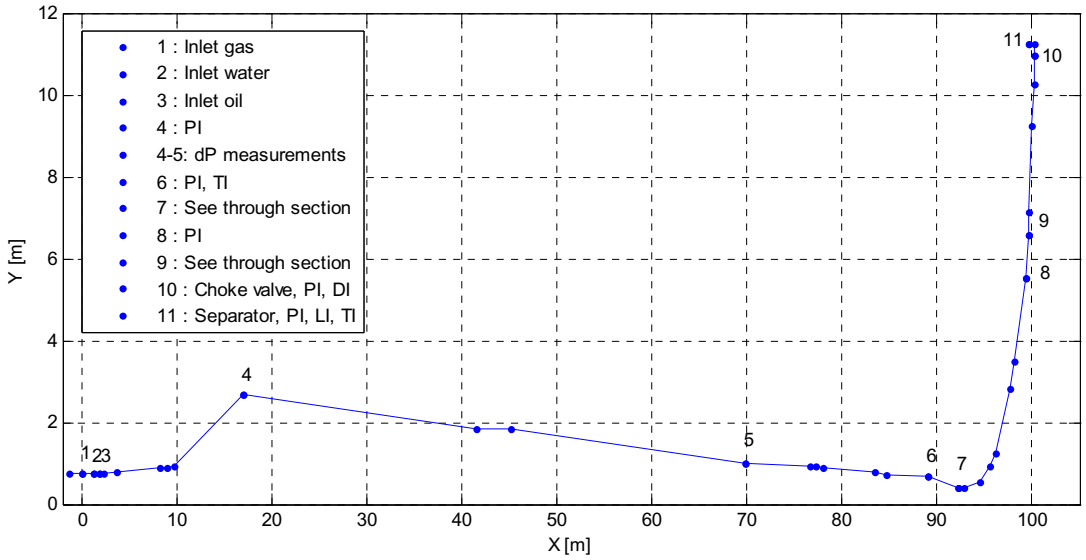
1 : Inlet gas
2 : Inlet water
3 : Inlet oil
4 : PI
4-5: dP measurements
6 : PI, TI
7 : See through section
8 : PI
9 : See through section
10 : Choke valve, PI, DI
11 : Separator, PI, LI, TI
Y [m]
X [m]
0
2
4
6
8
10
12
0
10
20
30
40
50
60
70
80
90
100
1
2
3
4
5
6
7
8
9
10
11

Figure 4

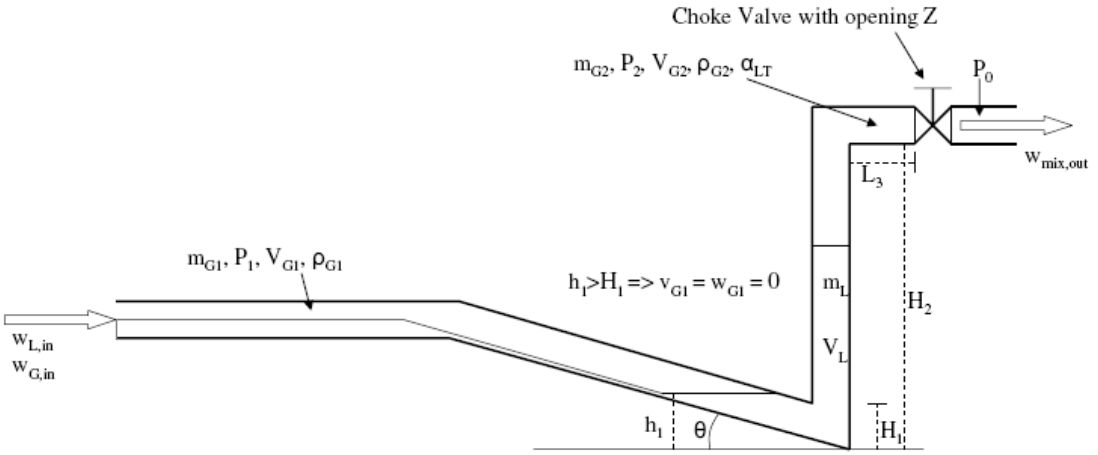

(a) Simplified representation of riser slugging

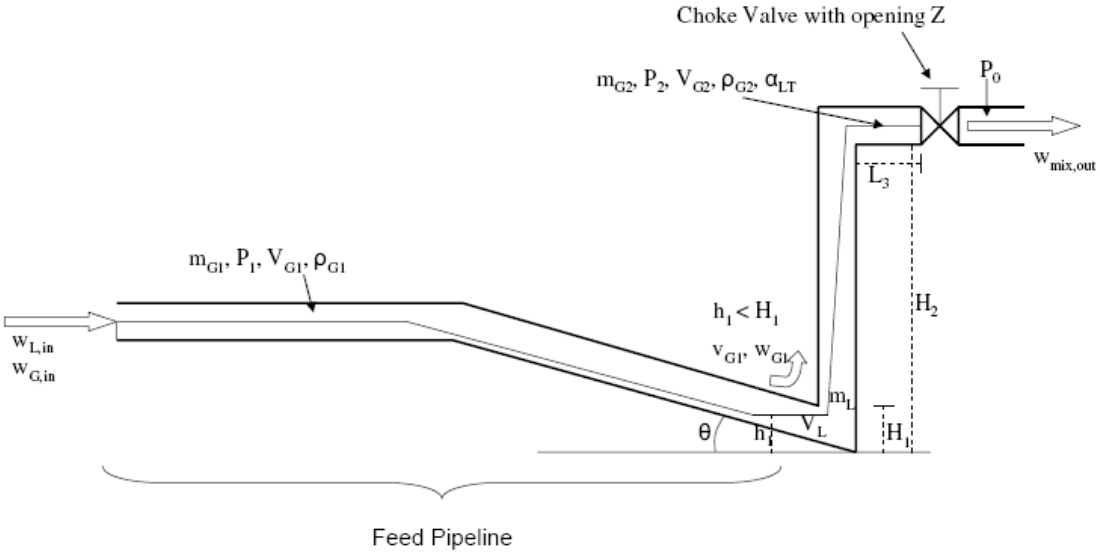

(b) Simplified representation of desired flow regime

Figure 5

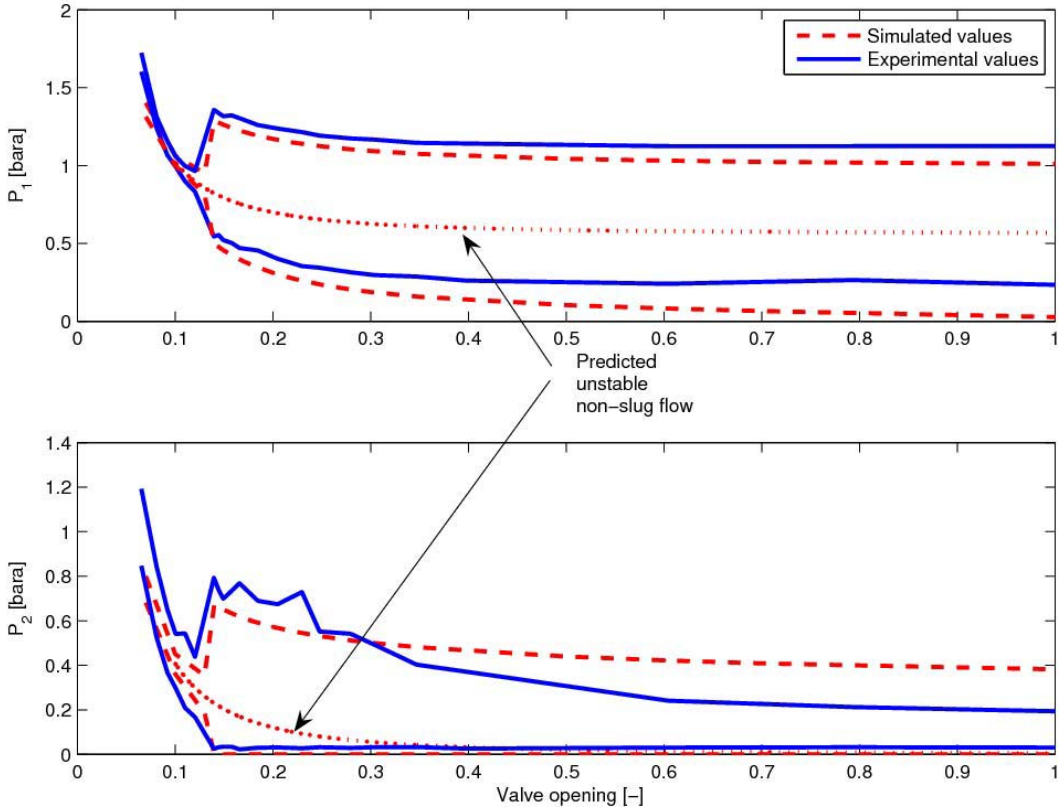
Simulated values
Experimental values
P1 [bara]
P2 [bara]
Predicted
unstable
non–slug flow
Valve opening [–]

Figure 6

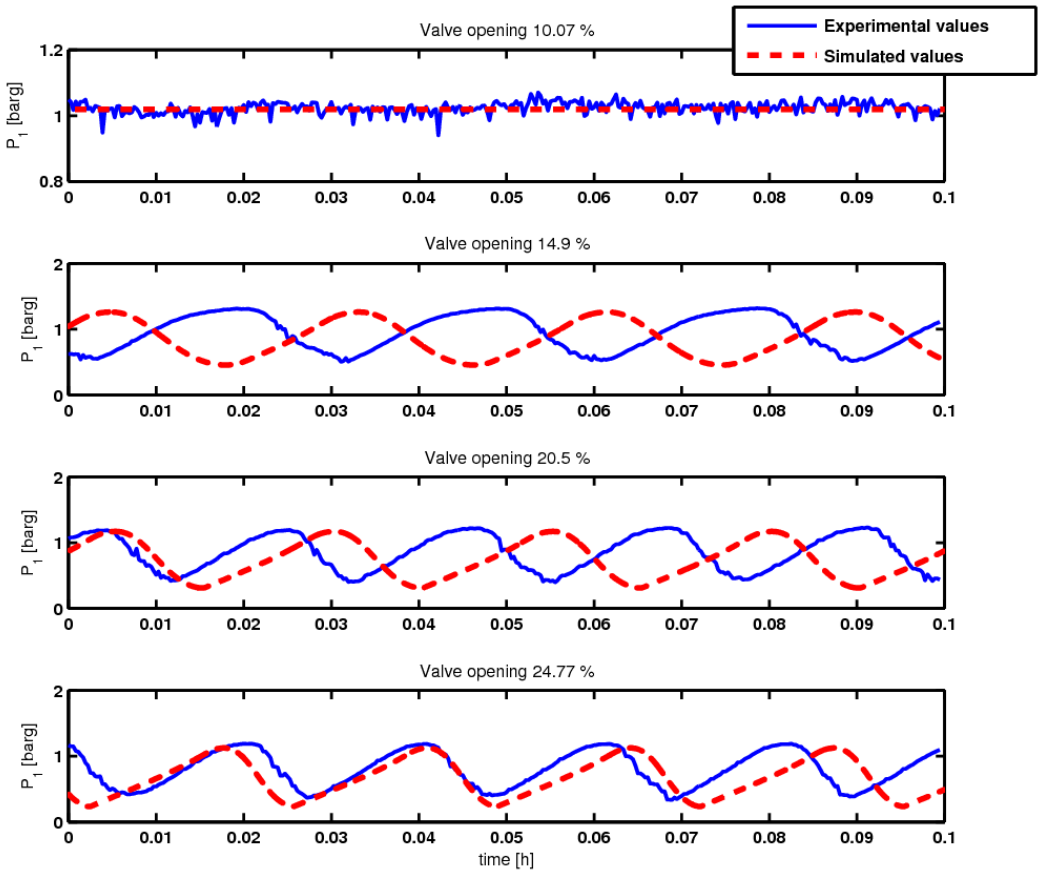
Experimental values
Simulated values
Valve opening 10.07 %
Valve opening 14.9 %
Valve opening 20.5 %
Valve opening 24.77 %
P1 [barg]
time [h]

Figure 7

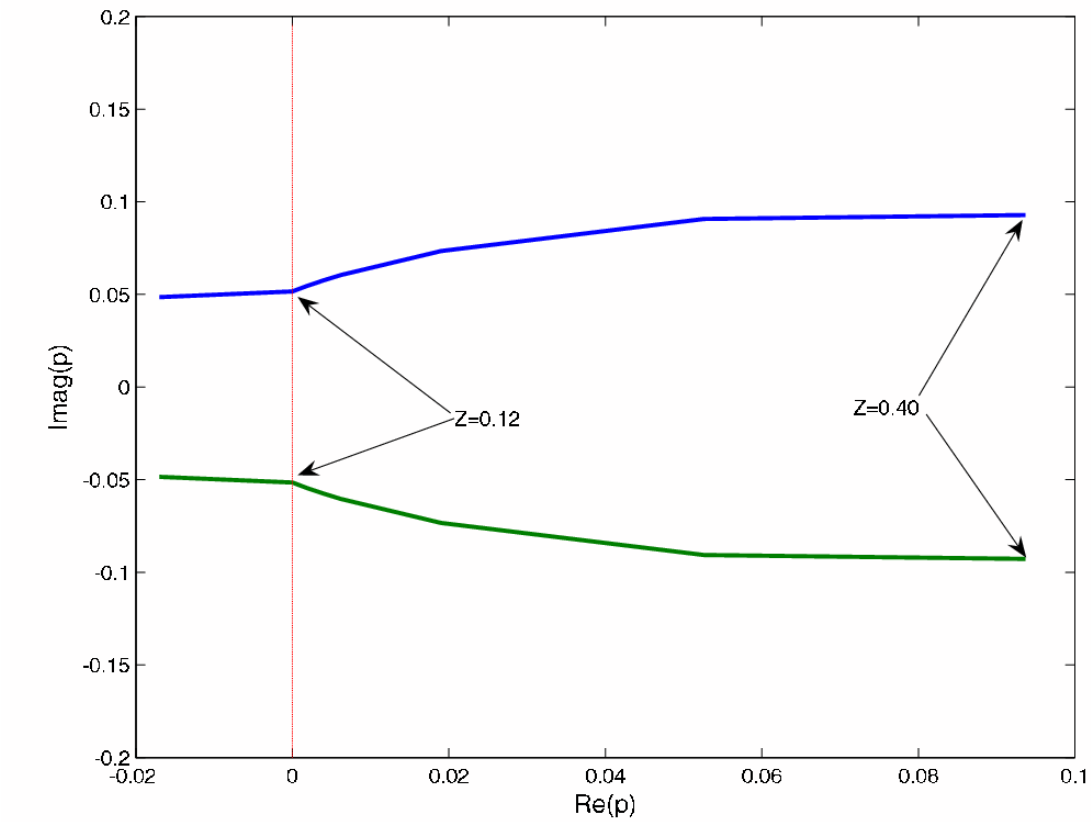
0.2
0.15
0.1
0.05
0
-0.05
-0.1
-0.15
-0.2
-0.02
0
0.02
0.04
0.06
0.08
0.1
Imag(p)
Re(p)
Z=0.12
Z=0.40

Figure 8

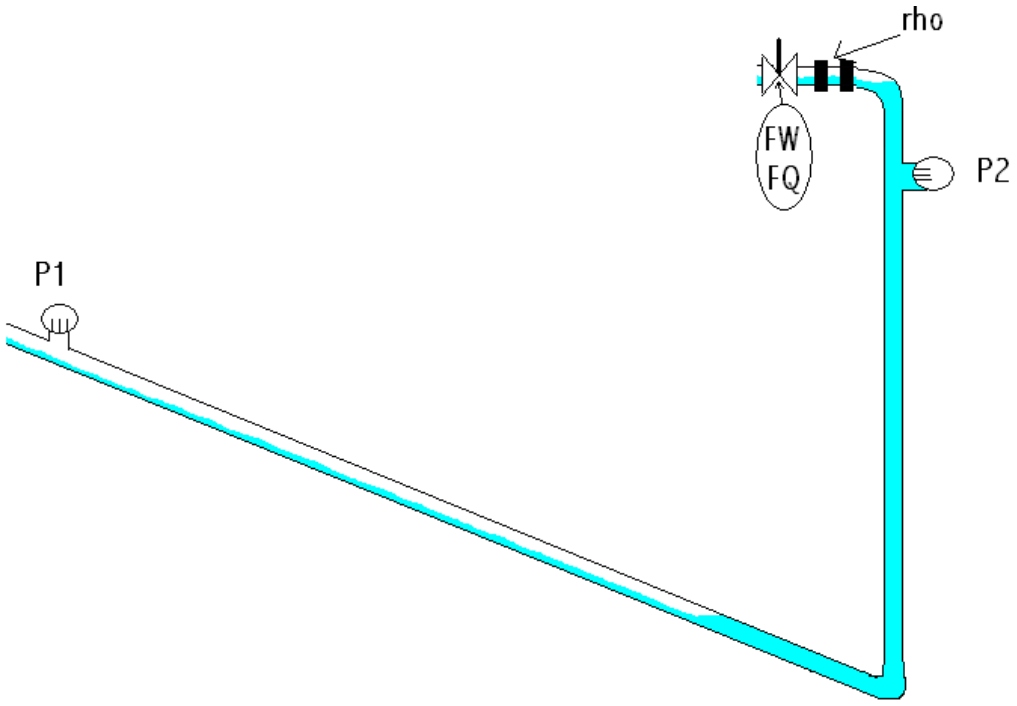

Figure 9

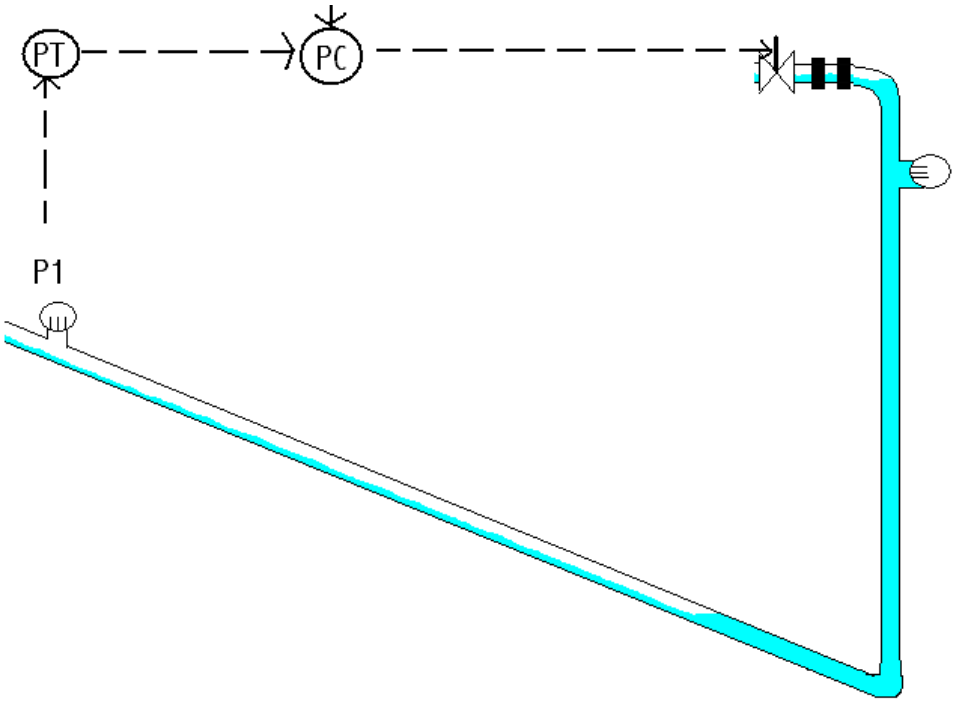

Figure 10

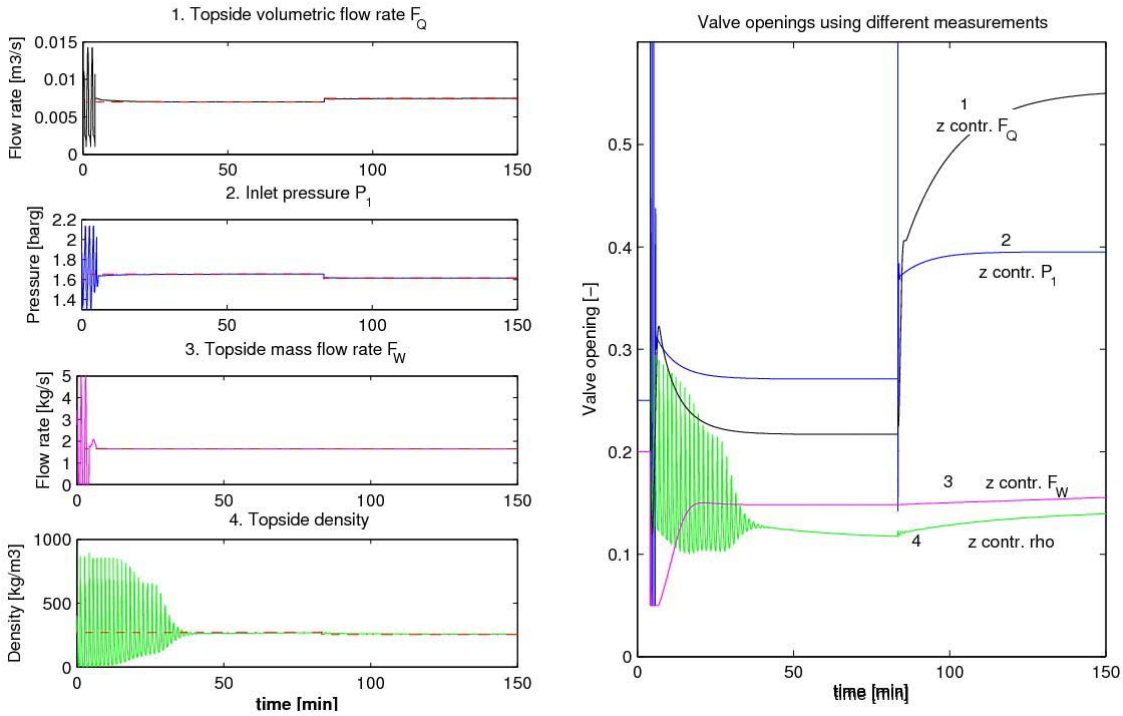
1. Topside volumetric flow rate F_Q
Flow rate [m3/s]
0.015
0.01
0.005
0
0
50
100
150
2. Inlet pressure P_1
Pressure [barg]
2.2
2
1.8
1.6
1.4
3. Topside mass flow rate F_W
Flow rate [kg/s]
5
4
3
2
1
4. Topside density
Density [kg/m3]
1000
500
time [min]
Valve openings using different measurements
Valve opening [–]
0.5
0.4
0.3
0.2
0.1
1
z contr. F_Q
2
z contr. P_1
3
z contr. F_W
4
z contr. rho
time [min]

Figure 11

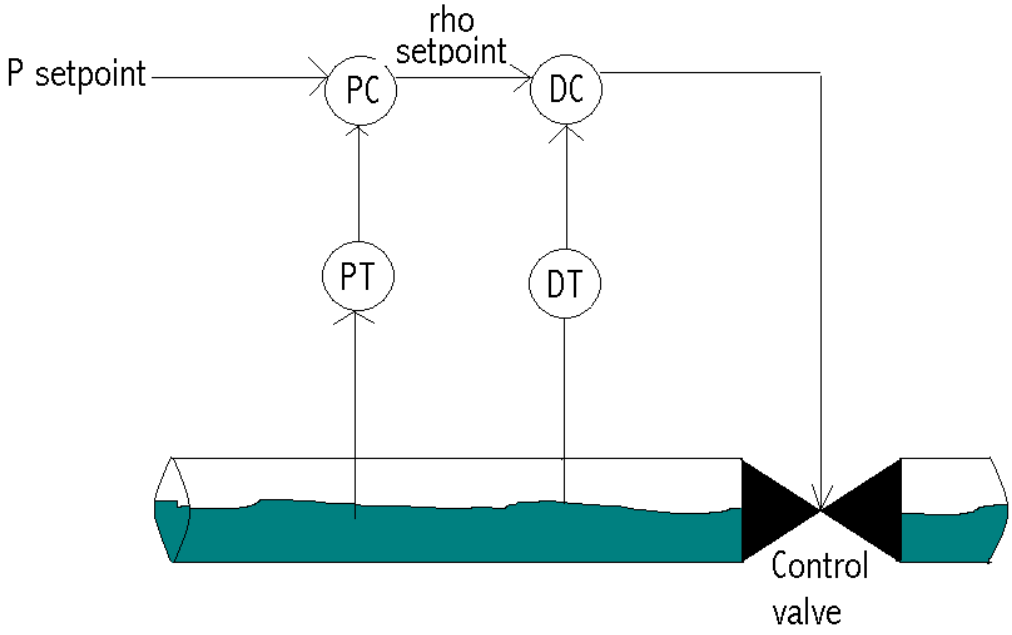

Figure 12 a

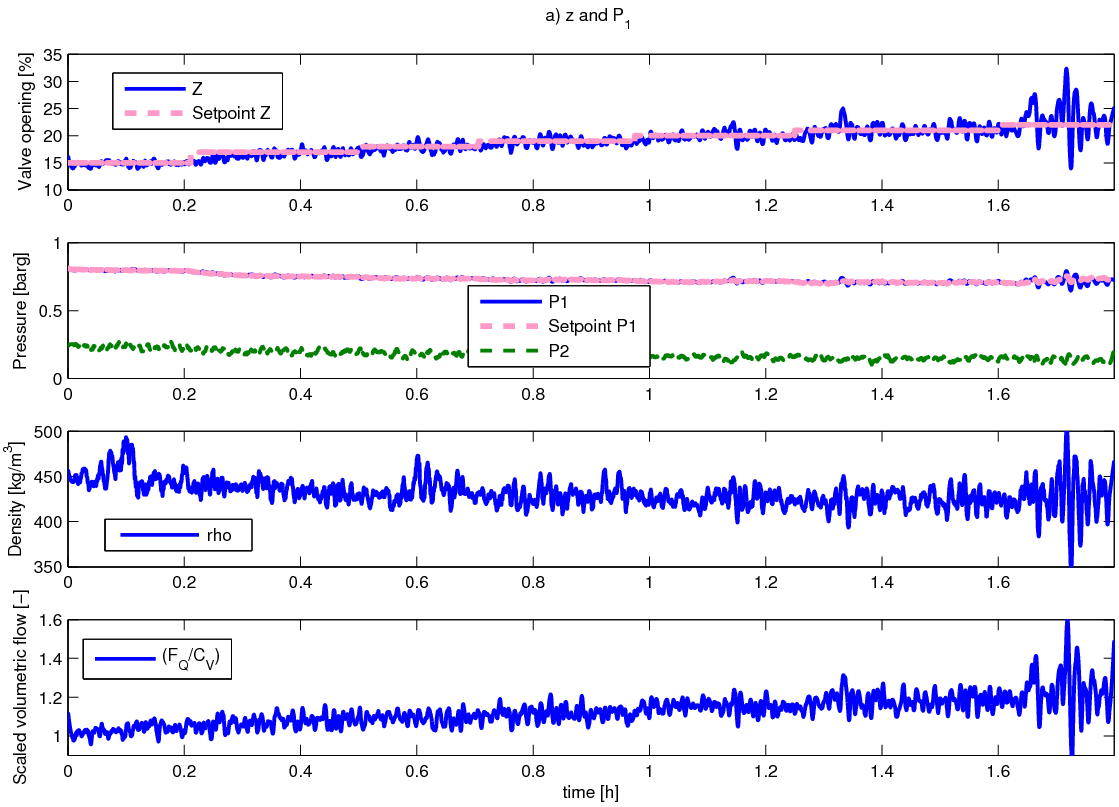
a) z and P1
Valve opening [%]
Z
Setpoint Z
Pressure [barg]
P1
Setpoint P1
P2
Density [kg/m3]
rho
Scaled volumetric flow [–]
(FQ/CV)
time [h]

Figure 12 b

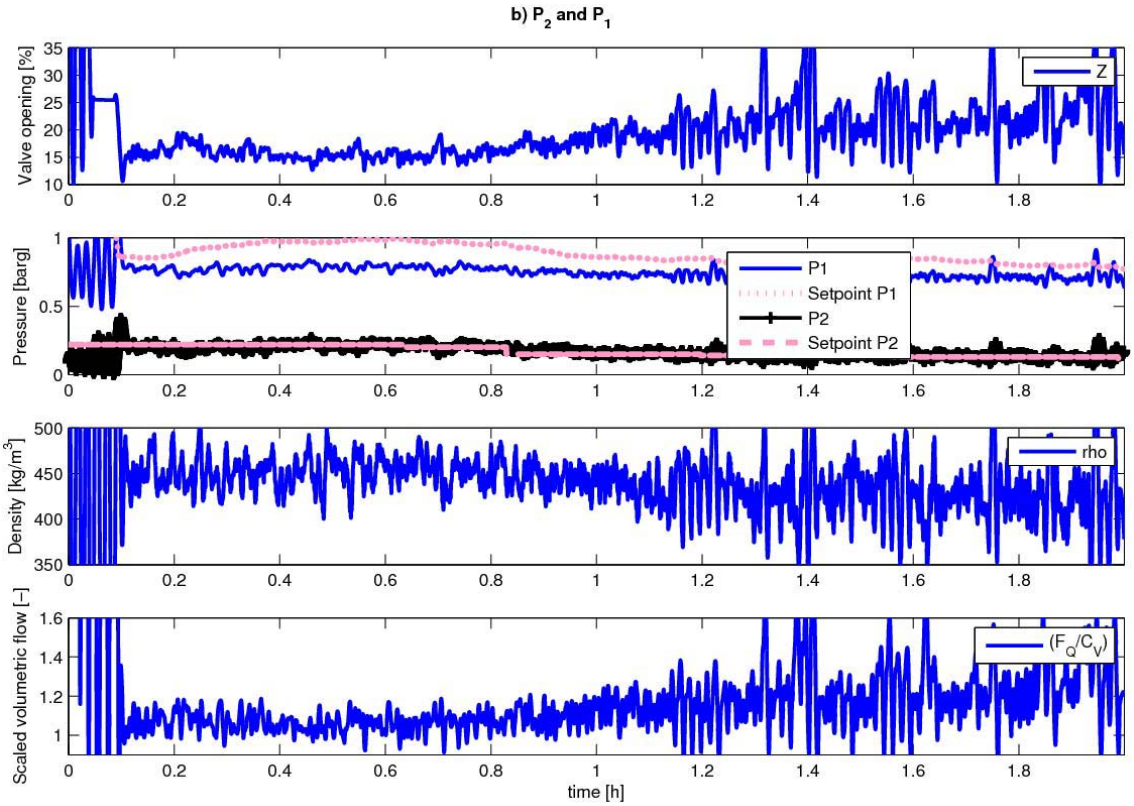
b) P2 and P1
Valve opening [%]
Z
Pressure [barg]
P1
Setpoint P1
P2
Setpoint P2
Density [kg/m3]
rho
Scaled volumetric flow [-]
(FQ/CV)
time [h]

Figure 13 a

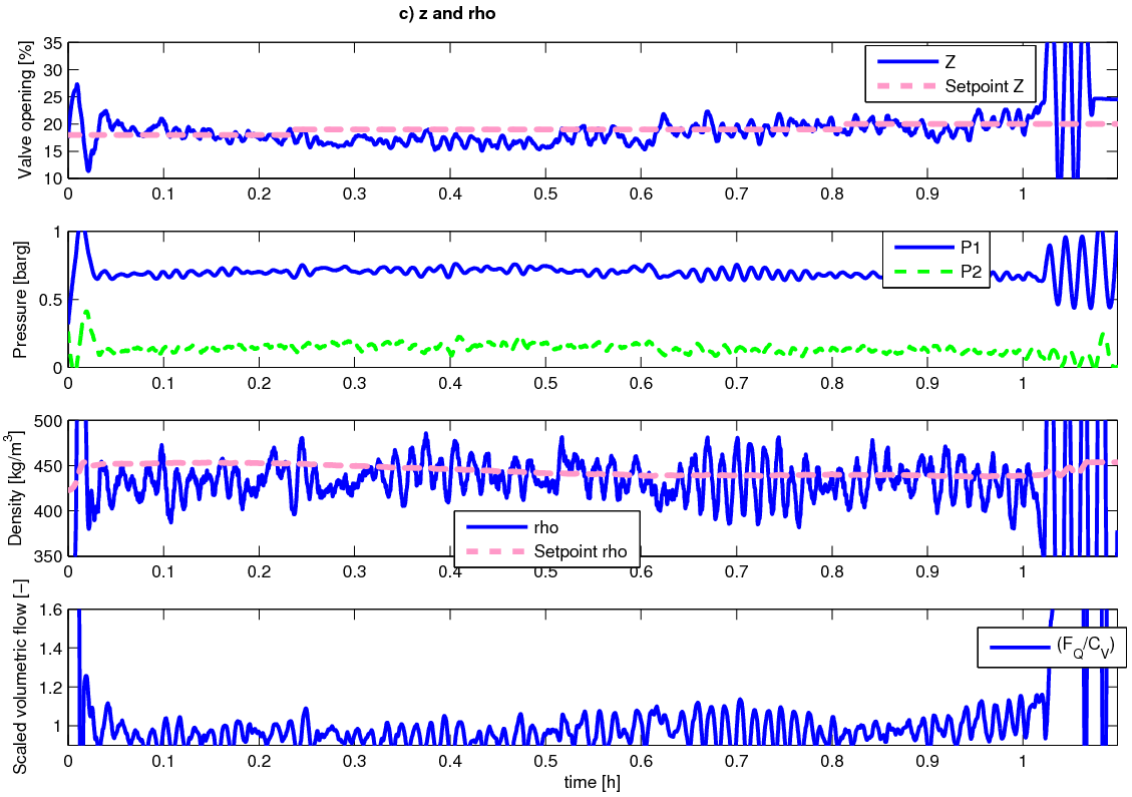
c) z and rho
Valve opening [%]
Z
Setpoint Z
Pressure [barg]
P1
P2
Density [kg/m3]
rho
Setpoint rho
Scaled volumetric flow [–]
(FQ/CV)
time [h]

Figure 13 b

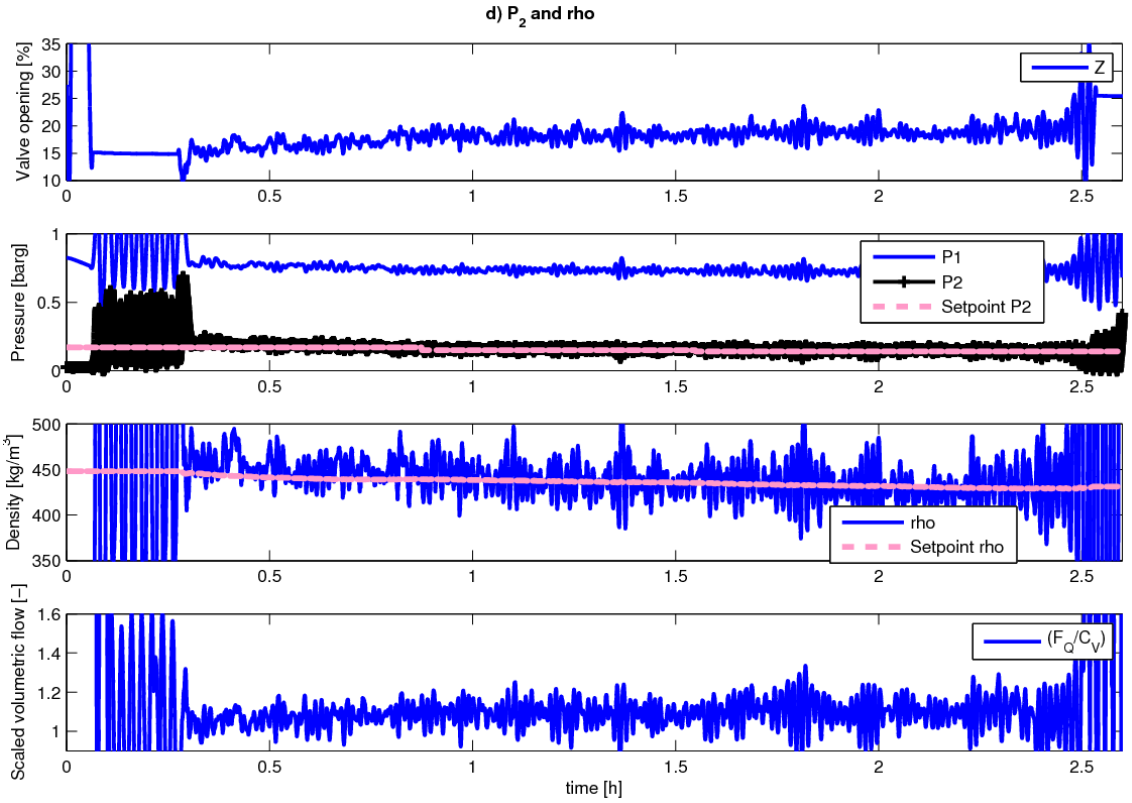
d) P2 and rho
Valve opening [%]
Z
Pressure [barg]
P1
P2
Setpoint P2
Density [kg/m3]
rho
Setpoint rho
Scaled volumetric flow [-]
(FQ/CV)
time [h]

Figure 14a

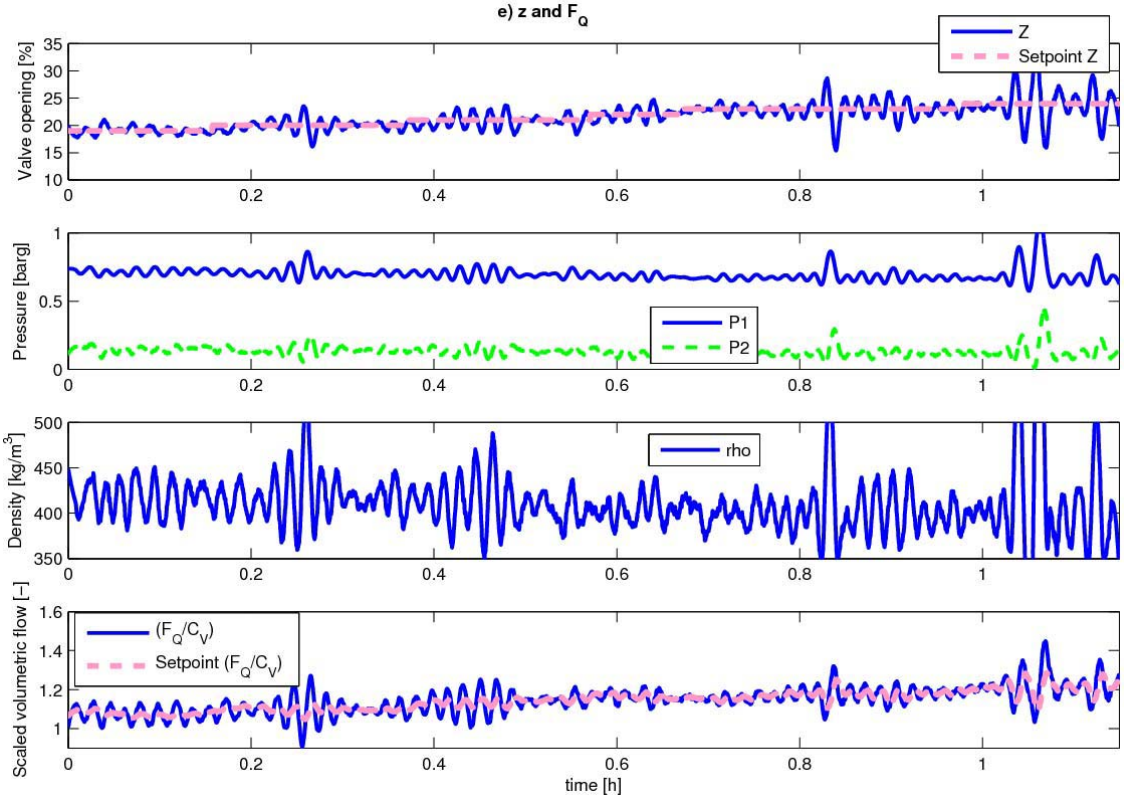
e) z and F_Q
Z
Setpoint Z
Valve opening [%]
P1
P2
Pressure [barg]
rho
Density [kg/m^3]
(F_Q/C_V)
Setpoint (F_Q/C_V)
Scaled volumetric flow [–]
time [h]

Figure 14 b

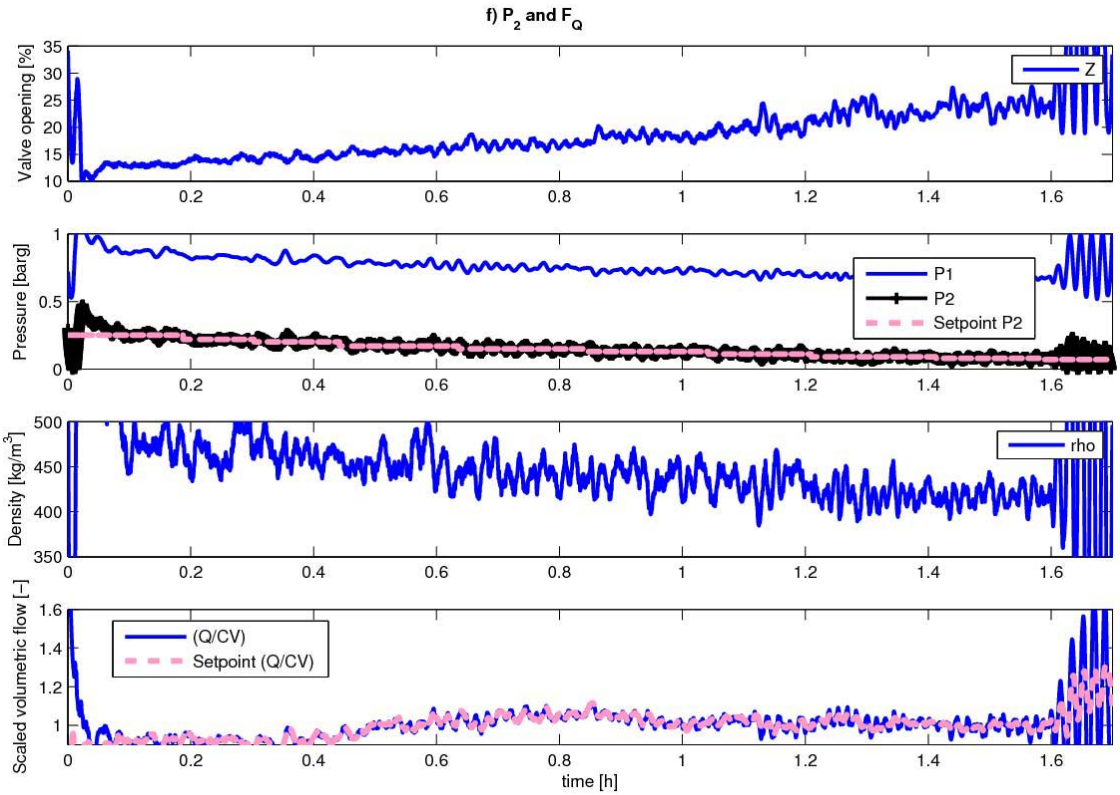
f) P2 and FQ
Valve opening [%]
Z
Pressure [barg]
P1
P2
Setpoint P2
Density [kg/m3]
rho
Scaled volumetric flow [-]
(Q/CV)
Setpoint (Q/CV)
time [h]

Figure A-1

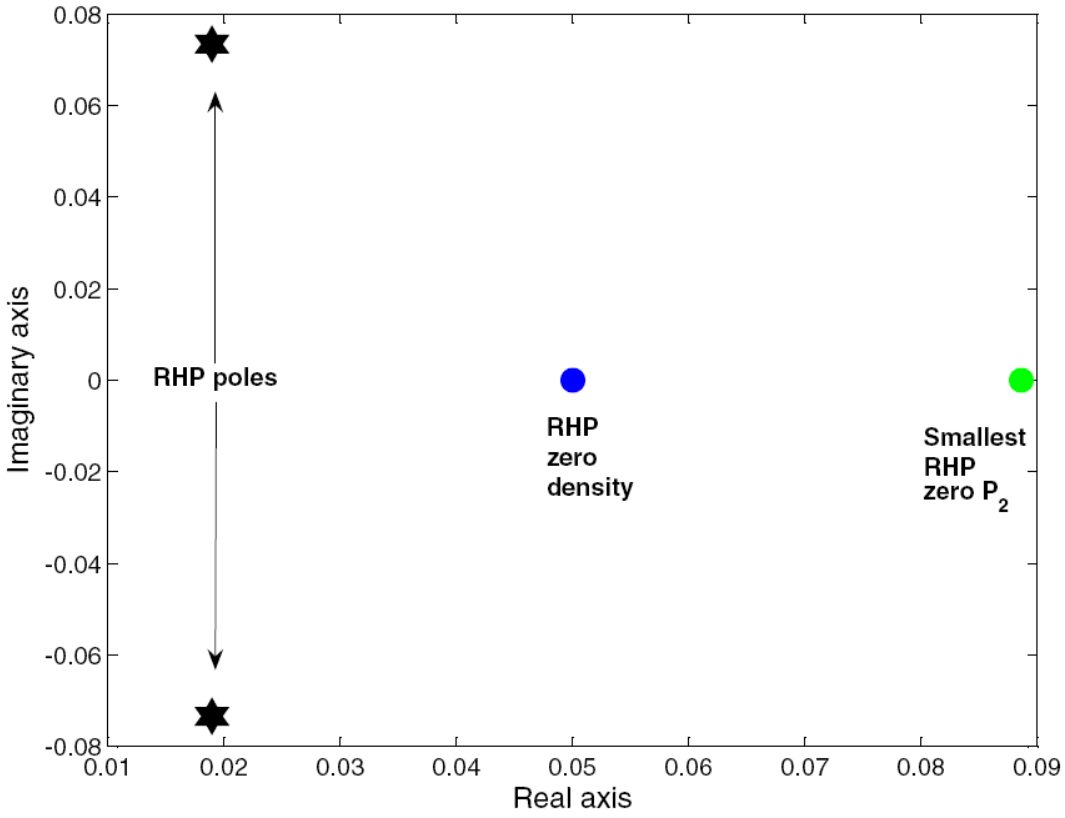
0.08
0.06
0.04
0.02
0
-0.02
-0.04
-0.06
-0.08
Imaginary axis
RHP poles
RHP
zero
density
Smallest
RHP
zero P2
0.01
0.02
0.03
0.04
0.05
0.06
0.07
0.08
0.09
Real axis

Figure A-2

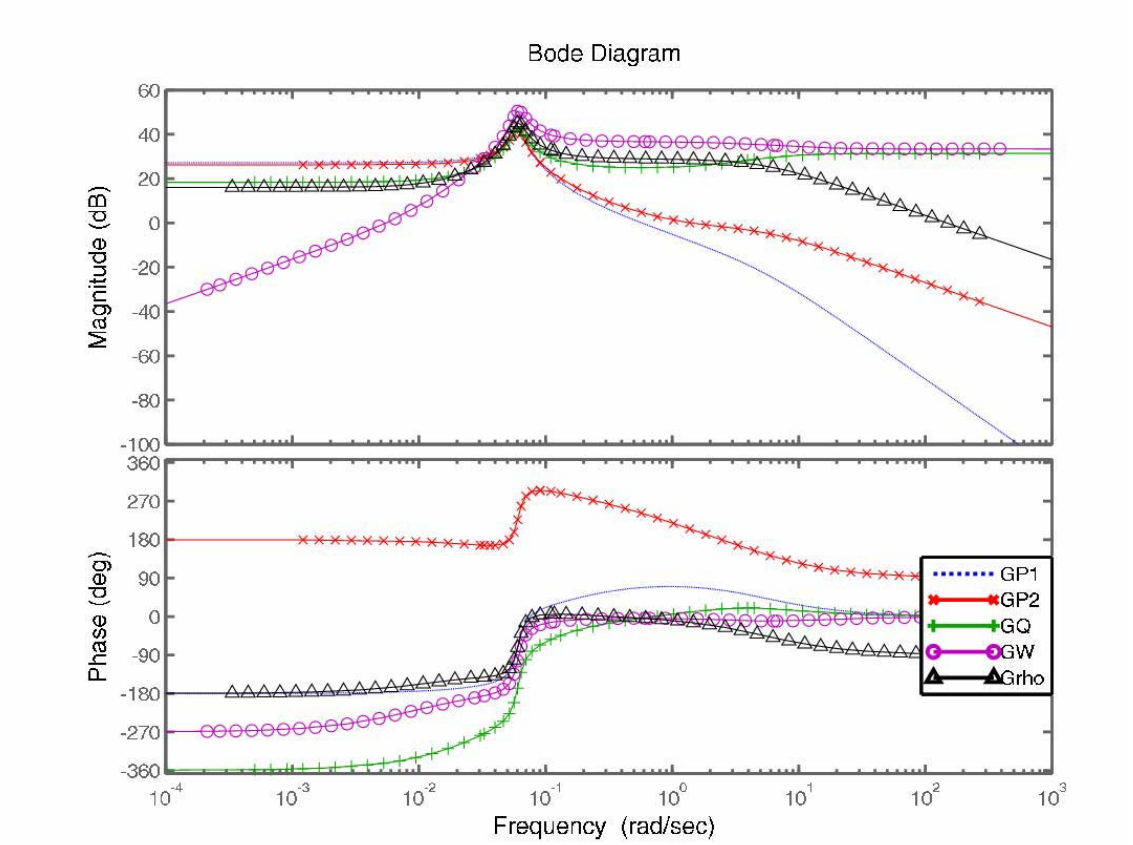
Bode Diagram
Magnitude (dB)
Phase (deg)
Frequency (rad/sec)
GP1
GP2
GQ
GW
Grho

Figure A-3

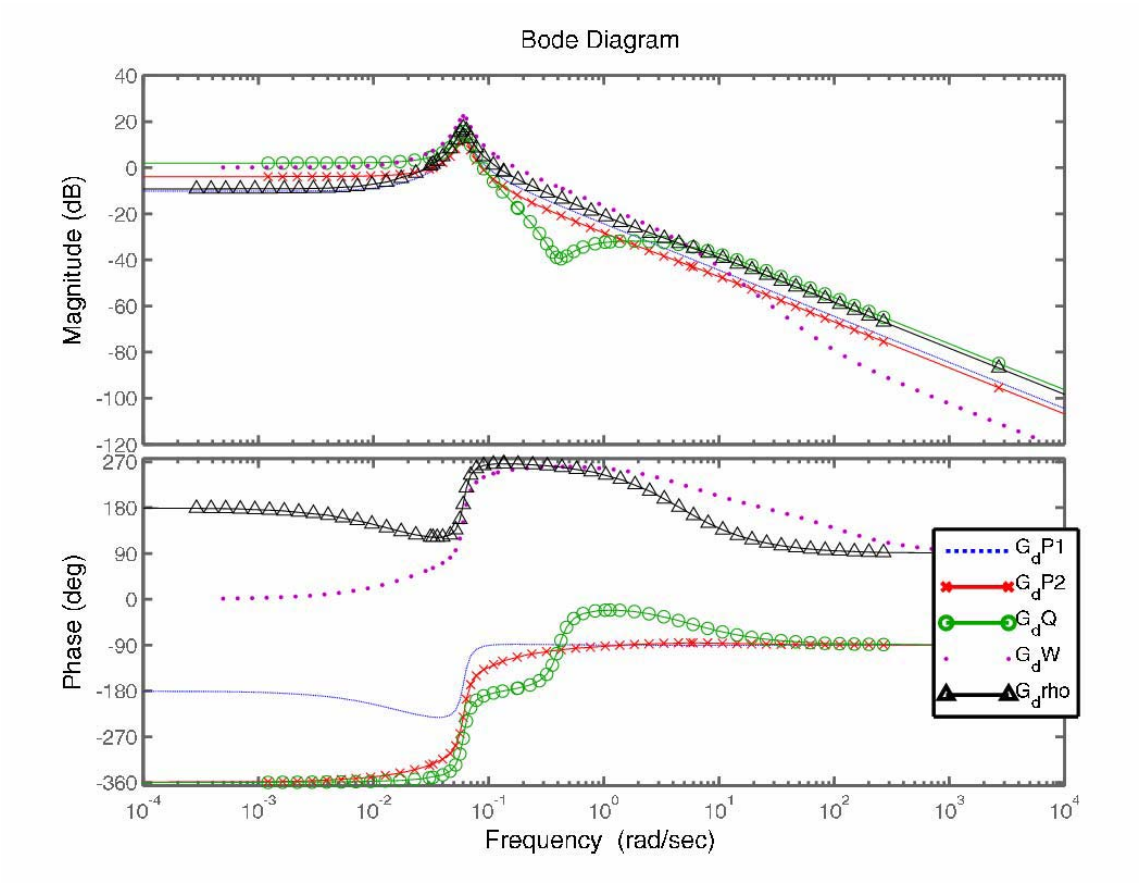
Bode Diagram
Magnitude (dB)
Phase (deg)
Frequency (rad/sec)
G_dP1
G_dP2
G_dQ
G_dW
G_drho

Figure B-1a

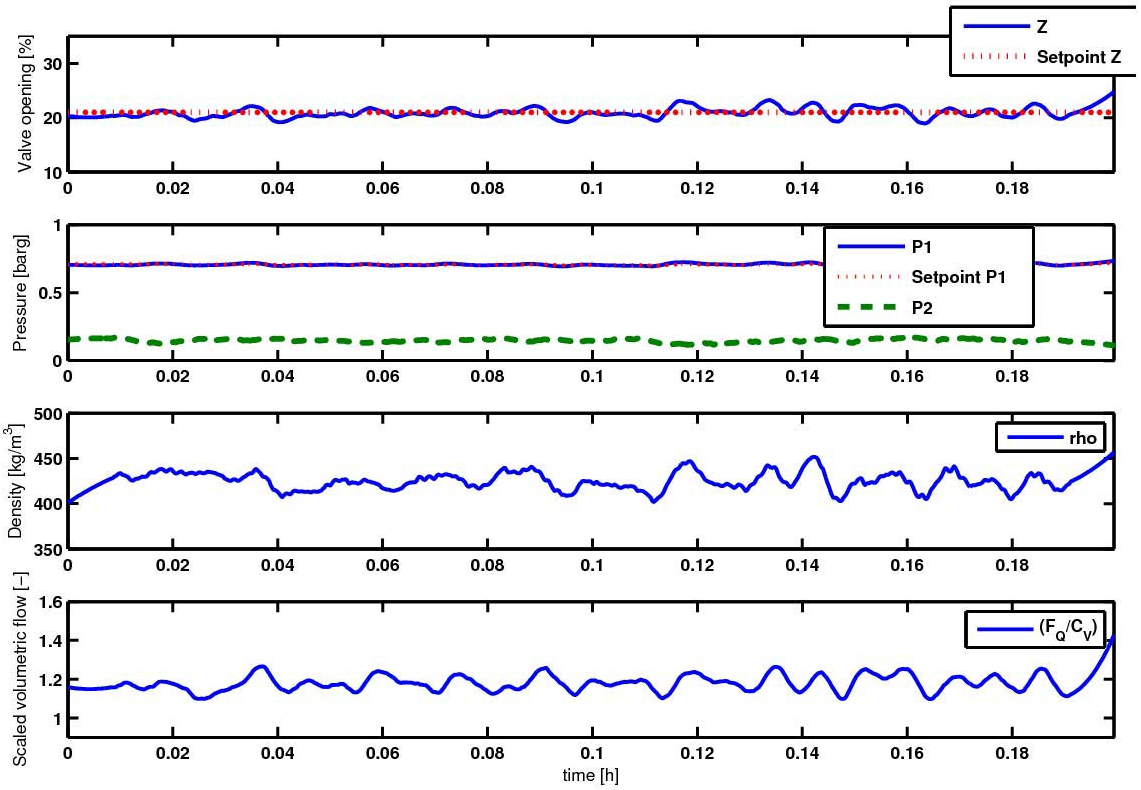
Valve opening [%]
Z
Setpoint Z
Pressure [barg]
P1
Setpoint P1
P2
Density [kg/m3]
rho
Scaled volumetric flow [–]
(FQ/CV)
time [h]

Figure B-1b

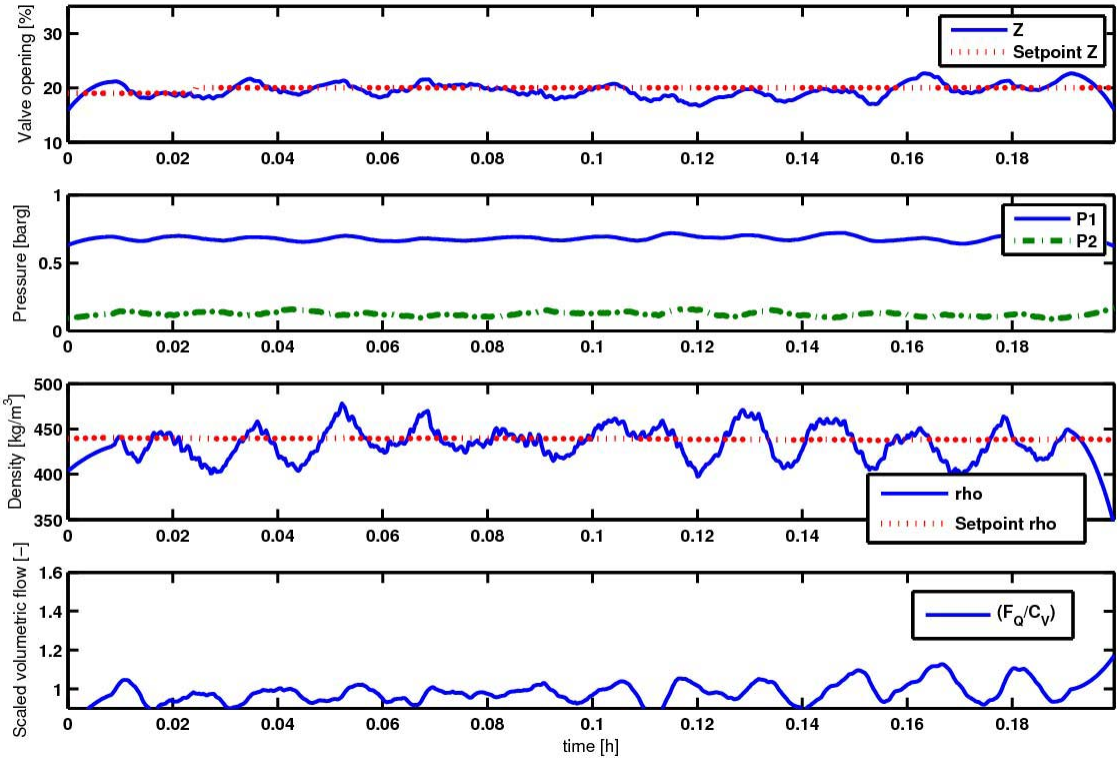
Valve opening [%]
Z
Setpoint Z
Pressure [barg]
P1
P2
Density [kg/m3]
rho
Setpoint rho
Scaled volumetric flow [–]
(FQ/CV)
time [h]

Figure B-1c

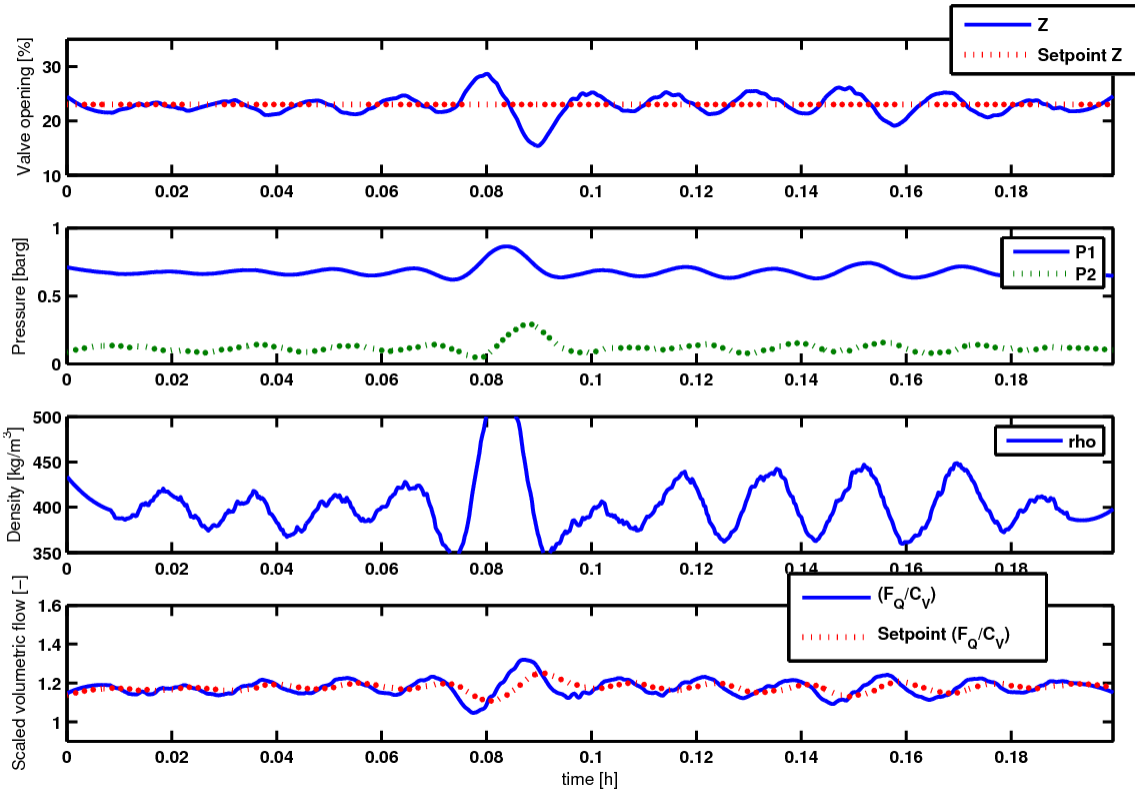
Z
Setpoint Z
Valve opening [%]
30
20
10
0
0.02
0.04
0.06
0.08
0.1
0.12
0.14
0.16
0.18
P1
P2
Pressure [barg]
1
0.5
0
rho
Density [kg/m3]
500
450
400
350
(FQ/CV)
Setpoint (FQ/CV)
Scaled volumetric flow [–]
1.6
1.4
1.2
1
time [h]

Figure B-1d

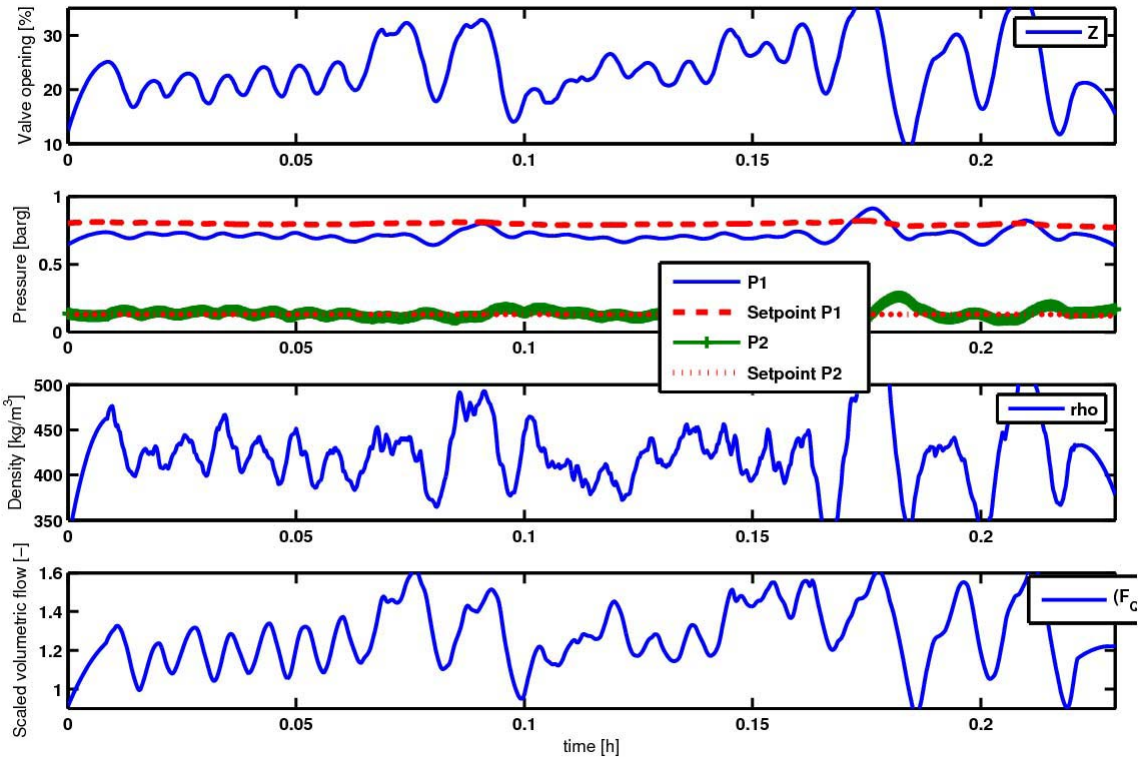
Valve opening [%]
30
20
10
0
0.05
0.1
0.15
0.2
Z
Pressure [barg]
1
0.5
0
P1
Setpoint P1
P2
Setpoint P2
Density [kg/m3]
500
450
400
350
rho
Scaled volumetric flow [–]
1.6
1.4
1.2
1
time [h]

Figure B-1e

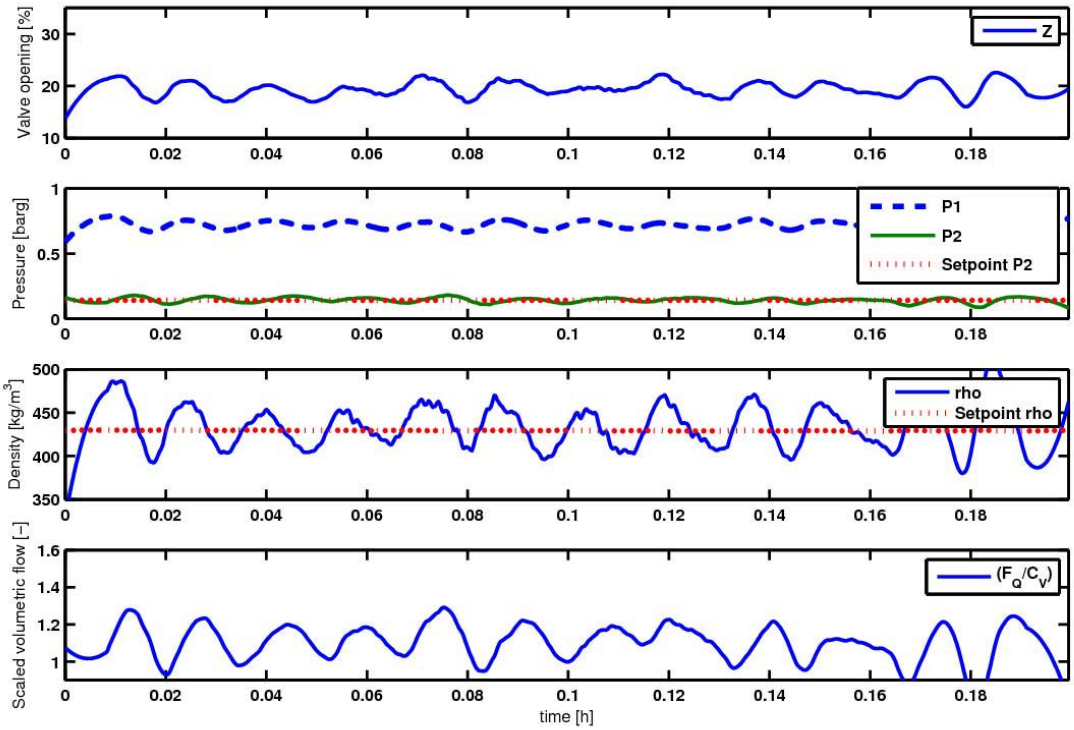
Valve opening [%]
Z
Pressure [barg]
P1
P2
Setpoint P2
Density [kg/m3]
rho
Setpoint rho
Scaled volumetric flow [–]
(FQ/CV)
time [h]

Figure B-1 f

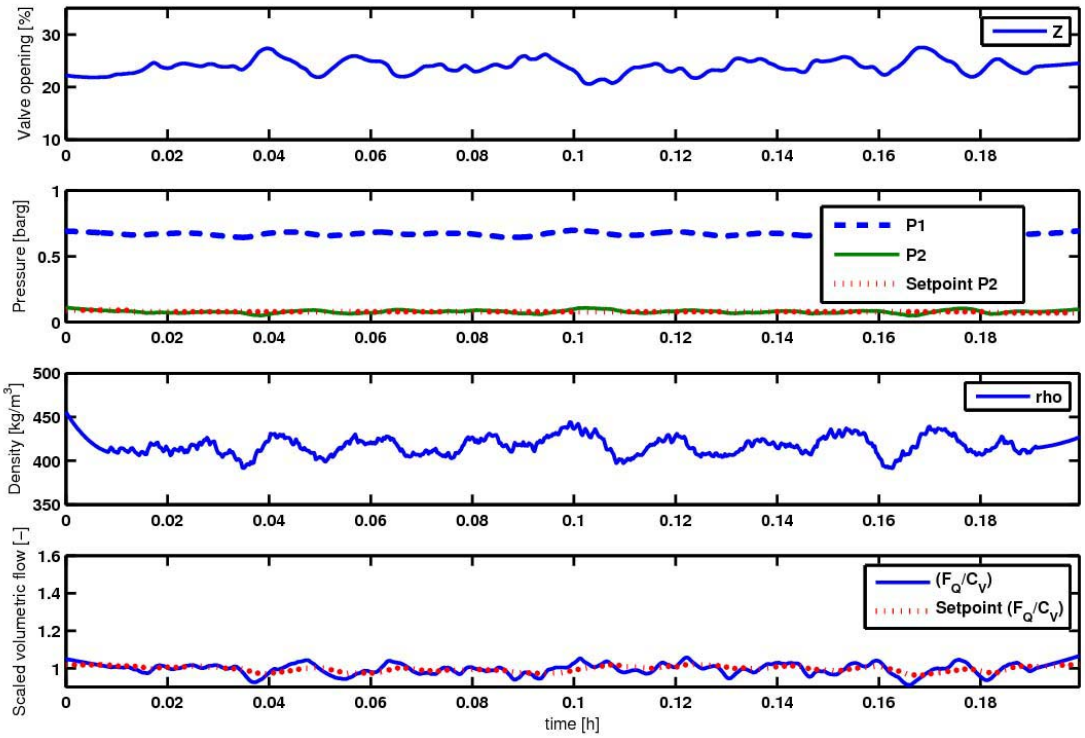
Valve opening [%]
Z
Pressure [barg]
P1
P2
Setpoint P2
Density [kg/m3]
rho
Scaled volumetric flow [-]
(FQ/CV)
Setpoint (FQ/CV)
time [h]

Tables:

Table 1 - Model data parameters

Parameter	**Symbol**	**Value**
Inlet flow rate gas [*kg/s*]	$w_{G,in}$	0.0075
Inlet flow rate water [*kg/s*]	$w_{L,in}$	1.644
Valve opening at bifurcation point [-]	z	0.12
Inlet pressure at bifurcationpoint [*barg*]	$P_{1,stasj}$	0.9
Topside pressure at bifurcationpoint [*barg*]	$P_{2,stasj}$	0.3
Separator pressure [*barg*]	P_0	0
Liquid level upstream low point at bifurcationpoint [*m*]	$h_{1,stasj}$	0.05
Upstream gas volume [m^3]	V_{G1}	0.2654
Feed pipe inclination [*rad*]	θ	0.05
Riser height [*m*]	H_2	10
Length of horizontal top section [*m*]	L_3	0.1
Pipe radius [*m*]	r	0.0381
Exponent in friction expression [-]	n	2.15
Choke valve constant [m^{-2}]	K_1	0.0042
Internal gas flow constant [-]	K_2	1.83
Friction parameter [s^2/m^2]	K_3	72.37

Table 2 - Mean values just before instability using different cascade controllers, based on data plotted in Figure B-1

Outer loop		**z**				**P_2**
Inner loop	**P_1**	**ρ**	**F_Q/C_v**	**P_1**	**ρ**	**F_Q/C_v**
P_1 [barg]	0.71	0.68	0.68	0.72	0.72	0.67
P_2 [barg]	0.146	0.123	0.119	0.132	0.142	0.079
ρ [kg/m^3]	425	433	403	424	433	417
F_Q/Cv[-]	1.18	0.98	1.18	1.28	1.094	0.997
z [%]	20.9	19.5	22.8	23.8	19.3	23.9
F_W [kg/h]	7.24	7.55	7.6	7.54	7.60	7.55
F_Q [m^3/h]	7.53	10.07	9.2	8.17	8.56	11.05
Figure	B-1 (a)	B-1 (b)	B-1 (c)	B-1 (d)	B-1 (e)	B-1 (f)

Table A-1 - Control limitation data for valve opening 15%. Unstable poles at p = 0.0062 ± 0.060i.

Measurement	RHP zeros	Stationary gain	Minimum bounds				
		|G(0)|	**|S|**	**|SG|**	**|KS|**	**|SGd|**	**|KSGd|**
P_1 [bar]	-	22.9	1.00	0.00	0.16	0.00	0.042
P_2 [bar]	1.00, 0.09	20.5	1.21	15.6	0.017	0.054	0.040
ρ [kg/m^3]	0.051	33.1	1.22	33.4	0.011	1.02	0.042
F_W [kg/s]	-	0.00	1.00	0.00	0.006	0.00	0.042
F_Q [m3/s]	-	8.3	1.00	0.00	0.013	1.02	0.040

Table A-2 - Control limitation data for valve opening 15%. Unstable poles at p = 0.019 ± 0.073i.

Measurement	RHP zeros	Stationary gain	Minimum bounds				
		|G(0)|	**|S|**	**|SG|**	**|KS|**	**|SGd|**	**|KSGd|**
P_1 [bar]	-	10.1	1.00	0.00	0.082	0.00	0.090
P_2 [bar]	1.08, 0.089	8.94	1.66	10.7	0.10	0.055	0.070
ρ [kg/m3]	0.050	2.87	1.60	19.6	0.048	1.27	0.080
F_W [kg/s]	-	0.00	1.00	0.00	0.021	0.00	0.070
F_Q [m3/s]	-	4.16	1.00	0.00	0.047	0.00	0.070